Contents lists available at ScienceDirect

Journal of Molecular Catalysis A: Chemical

journal homepage: www.elsevier.com/locate/molcata

NO reduction under diesel exhaust conditions over Au/Al$_2$O$_3$ prepared by deposition-precipitation method

P. Miquel[a,b], P. Granger[a], N. Jagtap[c], S. Umbarkar[c], M. Dongare[c], C. Dujardin[a,*]

[a] Université Nord de France, Université de Lille1, UCCS UMR8181 Bât C3, 59655 Villeneuve d'Ascq, France
[b] RENAULT SAS, Direction de l'Ingénierie des MATériaux, 91510 Lardy, France
[c] Catalysis and Inorganic Chemistry Division, National Chemical Laboratory, Pune 411008, India

ARTICLE INFO

ABSTRACT

Gold supported on alumina was prepared by urea deposition-precipitation method and compared to silver supported on alumina for the selective catalytic reduction of NO by hydrocarbons under lean conditions. The catalyst showed activity in the reduction of NO and 100% selectivity towards N$_2$ in the temperature range 300–350 °C. At higher temperature the NO conversion decreased due to competitive oxidative reactions of the reductants. XPS analysis confirmed the good stability of gold nanoparticles deposited on alumina. Infrared studies showed the formation of various adsorbed species (formates, carboxylates, ad-NO$_x$ and cyanide) on the catalyst surface. Addition of H$_2$ to the feed containing decane enhanced the formation of these species on the catalyst surface as well as the catalytic activity for the NO conversion to N$_2$.

1. Introduction

Lean burn automobile engines are becoming increasingly popular than the stoichiometric gasoline engines because of their high fuel efficiencies resulting in lower CO/CO$_2$ emissions. The actual three-way catalytic technology is inefficient under lean burn conditions for the reduction of NO$_x$ due to excess oxygen and lesser CO and hydrocarbon in the exhausts of these engines [1]. Up to now, various approaches and catalytic compositions have been investigated to reduce NO$_x$ from lean burn engines. In this context, NO$_x$ storage and reduction (NSR) developed by Toyota [2,3] and selective catalytic reduction of NO$_x$ by urea (urea-SCR) are the leading technologies for NO$_x$ abatement, hydrocarbon-SCR (HC-SCR) is still investigated as an alternative approach considering the addition of extra reducing agents in the exhaust gas [4,5]. Indeed, HC-SCR could reduce the need for noble metals catalysts and avoid urea addition constraints, but would induce penalties on the fuel consumption. Amongst the various catalytic formulations earlier reported, silver on alumina shows promising activity for the selective reduction of NO$_x$ to N$_2$ by hydrocarbons under lean conditions especially in the presence of hydrogen [5]. However, deactivation of the catalyst due to SO$_2$ in the exhaust gases is one of the major limitations of this catalyst system for its practical applications and improvement

in sulfur tolerance has been achieved, to some extent, by modifying the alumina support [6]. Silver on alumina catalyst system is extensively studied and the mechanism of NO$_x$ reduction and deactivation of the catalyst in the presence of SO$_2$ is well understood by *in situ* studies.

Supported gold-based catalysts [7–14] are also one more set of catalysts which have been investigated for HC-SCR of NO$_x$. Ueda and Haruta [11] have carried out a study of gold supported on various metal oxides for HC-SCR and reported Au/Al$_2$O$_3$ to be the most active in the reduction of NO$_x$ to N$_2$ in the presence of moisture and oxygen amongst all studied Au systems [10,11]. Recently, Ilieva et al. [15,16] have reported reduction of NO$_x$ by CO with 100% selectivity to N$_2$ at 200 °C over gold supported on ceria-alumina mixed catalysts. However, the catalytic activity of Au/Al$_2$O$_3$ is low compared to Ag/Al$_2$O$_3$ catalyst for SCR of NO$_x$ using hydrocarbons and the Au system is not investigated to the same extent.

Previous investigations of HC-SCR on Au/Al$_2$O$_3$ were performed in the presence of alkanes, alkenes [11–13] or CO as reductant [15,16]. Studies of the influence of heavy hydrocarbons and/or H$_2$, which are critical for Ag/Al$_2$O$_3$ catalysts have not been reported so far on gold-based catalysts. Theses reductants, which are present or added in the exhausts of a diesel engine, could be a key parameter to activate the reduction of NO$_x$ on Au/Al$_2$O$_3$ under lean conditions.

In the present paper, we have investigated the catalytic activity of Au/Al$_2$O$_3$ (1 wt.% Au) for HC-SCR of NO$_x$ under real diesel engine exhaust conditions and compared these results with those obtained on Ag/Al$_2$O$_3$ system. The presence of coexisting gases on

the catalytic activity of Au/Al$_2$O$_3$ for the selective reduction of NO as well as the effect of H$_2$ addition on the activity of these catalysts was also studied. Detailed *in situ* IR experiments were performed using hydrocarbons and hydrogen to investigate the nature of surface species formed during the course of the reaction to understand the mechanistic aspects of SCR of NO$_x$ over Au/Al$_2$O$_3$ catalyst.

2. Experimental

2.1. Preparation

γAl$_2$O$_3$ was obtained by sol–gel method using alkoxide precursors [17]. Before calcination, gold was deposited on alumina precursor by deposition-precipitation method using urea. Urea solution was heated at 80 °C and the solution of gold (III) chloride hydrate (HAuCl$_4$ aq) was added. Al$_2$O$_3$ precursor powder was then introduced after 5 min under stirring at 80 °C. The obtained sample was washed using water and dried at 80 °C. After subsequent drying, the sample (1 wt.% Au/Al$_2$O$_3$) was calcined in air at 500 °C for 12 h.

For comparison, silver-based catalyst was prepared by wet impregnation using silver nitrate salt as the precursor with the same alkoxide alumina precursor. Final catalyst (2 wt.% Ag/Al$_2$O$_3$) was obtained after successive drying overnight at 80 °C followed by calcination at 500 °C for 12 h.

2.2. Catalytic activity measurements

Temperature-programmed experiments were performed in a fixed-bed flow reactor. The reaction mixture was composed of 300 ppm NO, 300 ppm CO, 300 ppm C$_3$H$_6$, 0–100 ppm C$_{10}$H$_{22}$, 0–2000 ppm H$_2$, 10% O$_2$, 10% CO$_2$, 5% H$_2$O and balance He. The catalyst (300 mg) was used in a powder form (50–150 μm). The total flow rate of the gas mixture was set at 250 mL min^{-1} to obtain a gas hourly space velocity of 50,000 h^{-1}. The effluent gas was analyzed using an online mass spectrometer (Omnistar GSD 301) and a micro-GC (Varian CP 4900) fitted with thermal conductivity detectors. The reactants and products were separated on a molecular sieve 5 Å (NO, N$_2$, O$_2$, H$_2$ and CO) and a Poraplot Q column (N$_2$O, C$_3$H$_6$). C$_{10}$H$_{22}$ was monitored on the mass spectrometer. Prior to the reaction, the catalyst was submitted to similar thermal treatment as mentioned in Section 2.3.

2.3. Characterization of catalysts

IR spectra of the adsorbed species were recorded using a FTIR spectrometer (Thermo Nicolet 460 Protégé, MCT detector) equipped with a DRIFT cell (Harrick). Prior to each experiment, 30 mg of catalyst was heated in He flow at 385 °C at 10 °C min^{-1}. The sample was then cooled down to 128 °C (in the case of experiments with H$_2$) or 150 °C (experiments without H$_2$) under He flow and then heated again under the reaction mixture containing 467 ppm NO, 958 ppm CO, 958 ppm C$_3$H$_6$ and 173 ppm C$_{10}$H$_{22}$, 2000 ppm H$_2$ (when present), 5% O$_2$ with He. The ratio W/F_0 was also adjusted at 0.072 g s cm^{-3}.

Alternately, X-ray photoelectron spectroscopy (XPS) was used for the characterization of surface of fresh and used catalysts. XPS experiments were performed using a Vacuum Generators Escalab 220XL spectrometer equipped with an aluminum source for excitation in the analysis chamber under ultra high vacuum (10^{-10} Torr). Binding energy (B.E.) values were referenced to the binding energy of the Al 2p core level (74.6 eV) and quantification was carried out using CasaXPS software with Shirley background subtraction [18,19].
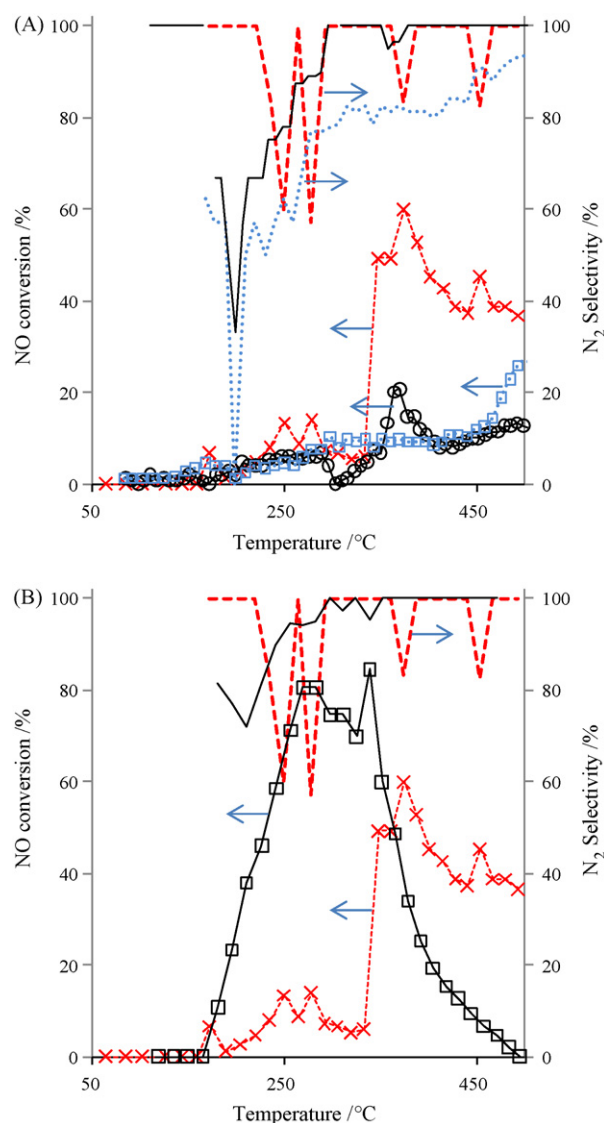
Fig. 1. Comparison of NO conversion and N$_2$ selectivity as a function of temperature over 1 wt.% Au/Al$_2$O$_3$ under NO + CO + C$_3$H$_6$ + C$_{10}$H$_{22}$ (circle), under NO + CO + C$_3$H$_6$ + H$_2$ (square) and under NO + CO + C$_3$H$_6$ + C$_{10}$H$_{22}$ + H$_2$ (cross) (A). Comparison of NO conversion and N$_2$ selectivity over 1 wt.% Au/Al$_2$O$_3$ and 2 wt.% Ag/Al$_2$O$_3$ in the presence of C$_{10}$H$_{22}$ and H$_2$ (B) (reaction conditions: 300 ppm NO, 300 ppm CO, 300 pm C$_3$H$_6$, 0 or 100 ppm C$_{10}$H$_{22}$, 0 or 2000 ppm H$_2$, 10% O$_2$, 10% CO$_2$, 5% H$_2$O and balance He.).

3. Results and discussion

3.1. HC-SCR of NO over 1 wt.% Au/Al$_2$O$_3$ and 2 wt.% Ag/Al$_2$O$_3$

The activated catalysts were exposed to reaction mixture on a fixed-bed reactor using 300 ppm NO, 300 ppm CO, 300 ppm C$_3$H$_6$, 0 or 100 ppm C$_{10}$H$_{22}$, 0 or 2000 ppm H$_2$, 10 vol.% O$_2$, 10 vol.% CO$_2$, 5 vol.% H$_2$O and balance He. Fig. 1(A) compares the activity of Au/Al$_2$O$_3$ as a function of temperature depending on the nature of the reductant. As observed, for the conversion curve recorded in the presence of CO, propylene and decane as reductants, two domains for the NO reduction are distinguished on Au/Al$_2$O$_3$. The first temperature domain (180–300 °C) shows a low conversion level (max. 7% conversion around 270–290 °C) accompanied with the production of N$_2$ and N$_2$O, the selectivity towards N$_2$ being higher than 66% above 210 °C. Above 320 °C, NO conversion increases till 20% at 370 °C and complete selectivity to N$_2$ is evidenced as previously reported over Au/Al$_2$O$_3$ [7]. The effect of hydrogen addition is first

Table 1
Temperature corresponding to 50% conversion of reductants on Au/Al_2O_3 and Ag/Al_2O_3 catalysts (300 ppm NO, 300 ppm CO, 300 ppm C_3H_6, 0–100 ppm $C_{10}H_{22}$, 0–2000 ppm H_2, 10% O_2, 10% CO_2, 5% H_2O and balance He).

Catalysts	Reductants	T_{50} CO (°C)	T_{50} H_2 (°C)	T_{50} C_3H_6 (°C)	T_{50} $C_{10}H_{22}$ (°C)
1 wt.% Au/Al_2O_3	$CO + C_3H_6 + C_{10}H_{22}$	480	–	357	359
	$CO + C_3H_6 + H_2$	<85	<85	375	–
	$CO + C_3H_6 + C_{10}H_{22} + H_2$	195	200	335	350
2 wt.% Ag/Al_2O_3	$CO + C_3H_6 + C_{10}H_{22} + H_2$	385	240	325	170

examined in the presence of CO and propylene as reductants, i.e. in the absence of decane. NO conversion remains below 10% until 420 °C. Activation of NO arises above 420 °C and reaches 26% at 500 °C, N_2 selectivity increasing with temperature. In presence of 2000 ppm H_2, the catalytic behavior of Au/Al_2O_3 is significantly promoted and, as previously observed, two conversion ranges are evidenced. The conversion level of NO previously observed above 350 °C increases significantly from 20 to 60% with a selectivity almost complete for N_2 while the low temperature conversion slightly changes. For comparison purposes a reference catalyst Ag/Al_2O_3 was chosen. Fig. 1(B) compares the NO reduction to N_2 and N_2O over 1 wt.% Au/Al_2O_3 and 2 wt.% Ag/Al_2O_3 in the presence of CO, propylene, decane and hydrogen. As previously described, two domains for the NO reduction are distinguished on Au/Al_2O_3 between 185 and 325 °C and above 350 °C, respectively. A classical behavior is reported in Fig. 1(B) for Ag/Al_2O_3 on HC-SCR. NO conversion begins at 170 °C and 75–85% of conversion is obtained in the temperature range of 250–350 °C. At the same time the selectivity to N_2 formation progressively increases with temperature till it reaches 100%.

The conversion of all the reductants (H_2, CO, C_3H_6 and $C_{10}H_{22}$) is measured during temperature-programmed experiments and temperatures corresponding to 50% of conversion are reported in Table 1 for both catalysts.

In the presence of CO, propylene and H_2, NO activation is delayed towards higher temperature whereas hydrogen as well as CO are highly consumed around 85 °C and propylene conversion increases from 280 to 500 °C. Clearly, two different phenomena proceed related to the oxidation of H_2 and CO at low temperature and the SCR of NO by propylene at higher temperature. A similar catalytic behavior of decane and propylene is observed in absence of H_2 with the activation of propylene and decane around 350 °C accompanied by NO conversion. In the presence of all reductants, H_2 and CO are activated on Au/Al_2O_3 at low temperature with T_{50} around 200 °C whereas no significant simultaneous reduction of NO arises in this temperature range. This is an indication that H_2 and CO are also non-selectively oxidized to H_2O and CO_2. By contrast, the activation of propylene and decane begins above 300 °C when the simultaneous reduction of NO to N_2 is evidenced. After 340 °C the NO conversion decreases progressively due to complete consumption of the reductants. The activation of reductants follows the sequence T_{50} $C_{10}H_{22}$ < T_{50} H_2 < T_{50} C_3H_6 < T_{50} CO on Ag/Al_2O_3. Clearly, decane combined to hydrogen addition seems to be the most efficient reductant mixture for the HC-SCR on both catalytic systems.
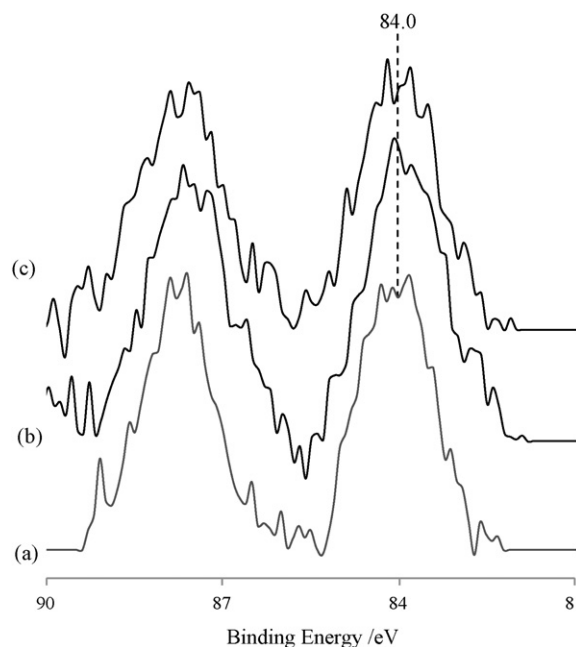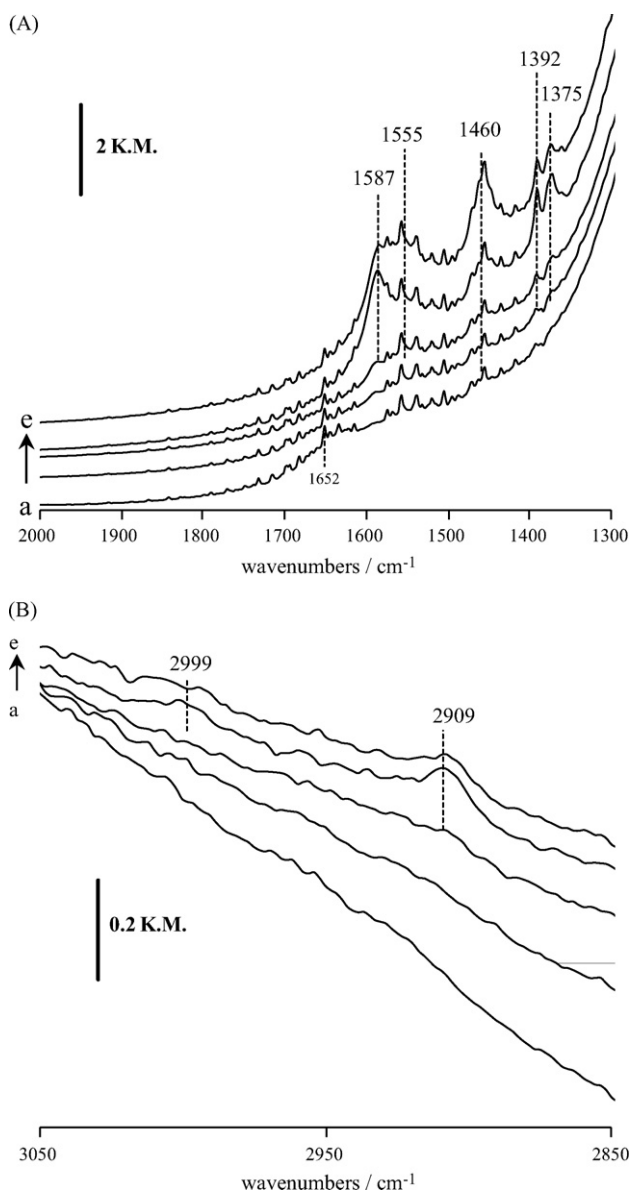

Fig. 2. Au 3f photopeak of Au/Al_2O_3 on fresh catalyst (a); after reaction under 300 ppm NO, 300 ppm CO, 300 ppm C_3H_6, 100 ppm $C_{10}H_{22}$, 10% O_2, 10% CO_2, 5% H_2O and balance He (b); after reaction under 300 ppm NO, 300 ppm CO, 300 ppm C_3H_6, 100 ppm $C_{10}H_{22}$, 2000 ppm H_2, 10% O_2, 10% CO_2, 5% H_2O and balance He (c).

3.2. Ex situ XPS measurements

Surface analysis was performed using XPS measurements. Fig. 2 shows the Au 3f photopeak before and after catalytic tests. On the fresh catalyst, the binding energy value of Au $3f_{7/2}$ photopeak is 84 eV, which is characteristic of metallic oxidation state of gold nanoparticles. After reaction under lean condition in the presence of decane (spectrum (b)) or in the presence of decane and hydrogen (spectrum (c)), the B.E. values do not vary significantly which confirms the preservation of the metallic character of gold nanoparticles even after high temperature treatment under excess of oxygen.

The surface concentration of Au is estimated from XPS measurements (Table 2). As observed, the Au/Al atomic ratio is not significantly altered after reaction varying within the margin of error. The stabilization of gold particles on alumina is evidenced

Table 2
Semi-quantitative analysis by XPS of 1 wt.% Au/Al_2O_3.

	B.E. Au $3f_{7/2}$ (eV)	FWHM[a] (eV)	Atomic ratio[b]	
			Au/Al	C/Al
Calcined	83.8	1.37	4.7×10^{-4}	0.15
After reaction in the absence of H_2[c]	84.1	1.48	6.3×10^{-4}	0.15
After reaction in the presence of 2000 ppm H_2[c]	84.2	1.42	5.3×10^{-4}	0.17

[a] Full width at half-maximum.
[b] Relative accuracy equal to 20%.
[c] 300 ppm NO, 300 ppm CO, 300 ppm C_3H_6, 100 ppm $C_{10}H_{22}$, 10% O_2, 10% CO_2, 5% H_2O and balance He.

(A)

(B)

Fig. 3. IR spectra of 1 wt.% Au/Al$_2$O$_3$ in temperature-programmed conditions with 467 ppm NO, 958 ppm CO, 958 ppm C$_3$H$_6$, 5% O$_2$ and balance He in the 1300–3000 cm^{-1} region. (a) 150 °C, (b) 185 °C, (c) 256 °C, (d) 343 °C and (e) 388 °C.

and no significant vaporization of gold can be evidenced even after ageing under reaction conditions at 500 °C. In addition the deposition of carbonaceous species is not observed on the catalyst surface (B.E. 285 eV) after the reaction (both in the absence or presence of hydrogen, Table 2).

3.3. In situ infrared studies

3.3.1. Infrared spectra over Au/Al$_2$O$_3$ under NO + CO + C$_3$H$_6$ + O$_2$

In order to identify the different species formed on the surface of the Au/Al$_2$O$_3$ during HC-SCR reactions, the catalyst placed in a DRIFT cell reactor was first exposed after successive pre-activation thermal treatment and cooling down at 150 °C to 467 ppm NO, 958 ppm CO, 958 ppm C$_3$H$_6$ and 5% O$_2$ with He as balance. Fig. 3 presents the IR spectra during the temperature-programmed sequence under reaction mixture. At 150 °C, the 1652 cm^{-1} IR band (spectrum a) reveals the presence of adsorbed water at the surface of the solid (Fig. 3A). Further increase in temperature leads to the appearance of IR bands located at 1587, 1460, 1392, 1375 cm^{-1}
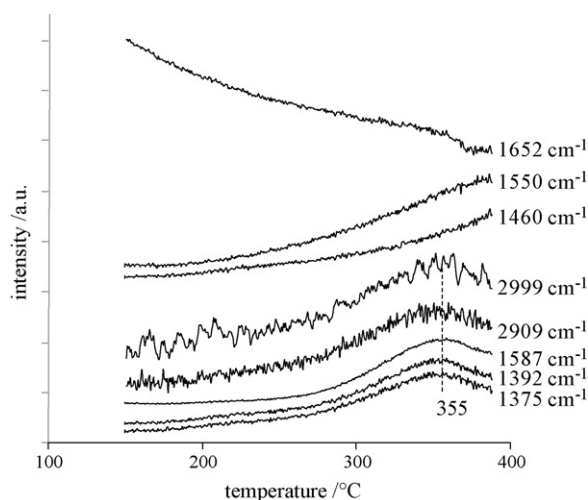
Fig. 4. Evolution of IR bands intensity of 1 wt.% Au/Al$_2$O$_3$ during temperature-programmed reaction with 467 ppm NO, 958 ppm CO, 958 ppm C$_3$H$_6$, 5% O$_2$ and balance He.

(Fig. 3A) and at 2999 and 2909 cm^{-1} (Fig. 3B). Finally, at 388 °C, a shoulder around 1555 cm^{-1} develops. The evolution of intensity is extracted as a function of temperature for all IR bands and is presented in Fig. 4. The evolution of bands located at 1375, 1392, 1587, 2909 and 2999 cm^{-1} follows the same trends with an increase in intensity until 355 °C and a progressive attenuation of their intensity above this temperature is observed. Clearly these IR bands arise from a unique adsorbed species assigned to formate species in agreement with previous IR studies [20] (Table 3).

At higher temperature, the 1460 and 1555 cm^{-1} IR bands develop. Several assignments can be proposed according to the literature data. The formation of carbonate with ν_s(COO) and ν_{as}(COO) modes, respectively, can arise from propylene oxidation at the surface of the catalyst. However, the evolution of intensity of the signal around 1555 cm^{-1} does not match exactly with the one of 1460 cm^{-1} band which can be associated with the signal around 1555 cm^{-1} and further tentatively assigned to nitrite linearly coordinated to alumina. Previous IR studies ascribed bands around 1460–1555 cm^{-1} to acetate adsorbed on alumina but the absence of signals corresponding to methyl group previously reported by Greenler [21] is not in agreement with this assignment in our present study.

3.3.2. Effect of decane addition

Decane was added to previous feed and IR spectra were recorded as a function of temperature (Fig. 5). The global features of IR spectra remain similar to that without the addition of C$_{10}$H$_{22}$. IR spectra evidence the development of band located at 1375, 1392, 1587, 2909 and 2999 cm^{-1} at intermediate temperature previously assigned to formate species. The development of carbonate species and nitrite species associated to signals at 1460 and 1555 cm^{-1} arises at high temperature (Fig. 5A). At low temperature, the appearance of new IR bands at 2960, 2929 and 2860 cm^{-1} can reflect the adsorption of decane on the surface of the catalyst (Fig. 5B). The evolution of intensities as a function of temperature is reported in Fig. 6. At low temperature, decane accumulates on the surface of the catalyst and desorbs/reacts as temperature increases. Formate species concentration reaches a maximum at 360 °C whereas carbonate species accumulate above 360 °C. Neither isocyanate nor cyanide species can be detected at any temperature under these conditions.

Table 3
Assignment of IR bands.

| Catalyst	Assignments	Vibrational modes	Wavenumbers (cm^{-1})	
			Literature [reference]	This study
Al$_2$O$_3$	Formate	$\nu_{(s)OCO}$	1380 [20]	1375
		$\nu_{(as)OCO}$	1595 [20]	1587
		δ_{CH}	1395 [20]	1392
		ν_{CH}	2905 [20]	2909
		$\nu_{(a)OCO} + \delta_{CH}$	2970 [20]	2999
Cu/SiO$_2$	Cu^0–NCO	ν_{NCO}	2230–2240 [22]	
	Cu^{2+}–NCO		2180–2185 [22]	
Au/SiO$_2$	Au–NCO	ν_{NCO}	2180–2186 [23]	2196
Ag/Al$_2$O$_3$	Al^{3+}–CN	ν_{CN}	2155 [24]	2180–2196
	Ag–CN		2127 [24]	2128–2152
Au/SiO$_2$	Au–NO$^-$	ν_{NO}	1733 [23]	1719
Co/ZrO$_2$	NO$_2$$^-$ (bridging nitro)	$\nu_{(as)NO_2}$	1545–1530 [25]	1555
Ag/Al$_2$O$_3$	NO$_3$$^-$ (nitrate B)	$\nu_{N=O}$	1580 [26]	1624
		$\nu_{(as)NO_2}$	1305 [26]	1308
Ag/Al$_2$O$_3$	Free carboxylate	$\nu_{(as)OCO}$	1575 [26]	1555
	COO$^-$/acetate	$\nu_{(s)OCO}$	1465 [26]	1457
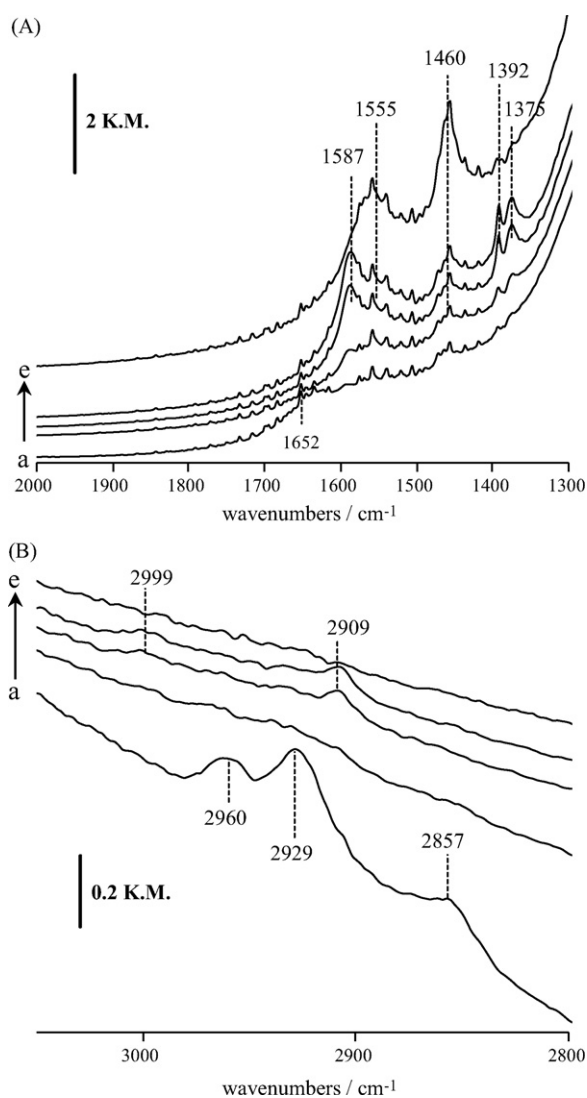
Fig. 5. IR spectra of 1 wt.% Au/Al$_2$O$_3$ in temperature-programmed conditions with 467 ppm NO, 958 ppm CO, 958 ppm C$_3$H$_6$, 173 ppm C$_{10}$H$_{22}$, 5% O$_2$ and balance He in the 1300–3000 cm^{-1} region. (a) 150 °C, (b) 250 °C, (c) 325 °C, (d) 363 °C and (e) 441 °C.

3.3.3. Effect of hydrogen and decane additions

Simultaneous addition of decane and hydrogen to initial feed was used for the characterisation of Au/Al$_2$O$_3$ during NO reduction with hydrocarbons. IR spectra of Au/Al$_2$O$_3$ catalyst and the evolution of band intensity vs. temperature are presented in Fig. 7 and Fig. 8, respectively.

By contrast to previous experiments, strong changes are mainly observed at low temperature (spectrum a) with the appearance of new bands at 2196, 1719, 1624, 1587 and 1308 cm^{-1} in addition to decane-related signals (2962, 2927 and 2857 cm^{-1}). The intensity of bands assigned to decane adsorption decreases progressively with increase in the temperature. Signals at 1719, 1624, 1587 and 1308 cm^{-1} also disappear until 250–350 °C. The adsorption of NO on gold particles (Au–NO or Au–NO$^-$) is evidenced with large band at 1719 cm^{-1} in the presence of hydrogen. Addition of hydrogen can prevent superficial oxidation of gold particles or accumulation of inhibiting species like adsorbed oxygen. The evolution of other IR bands with temperature is complex but we can isolate intense signals at 1624 and 1305 cm^{-1} with similar evolution and likely assigned to a nitrate species with $\nu_{(N=O)}$ and $\nu_{as(ON-O)}$ vibration modes, respectively. Additional signal of nitrite at 1587 cm^{-1} is
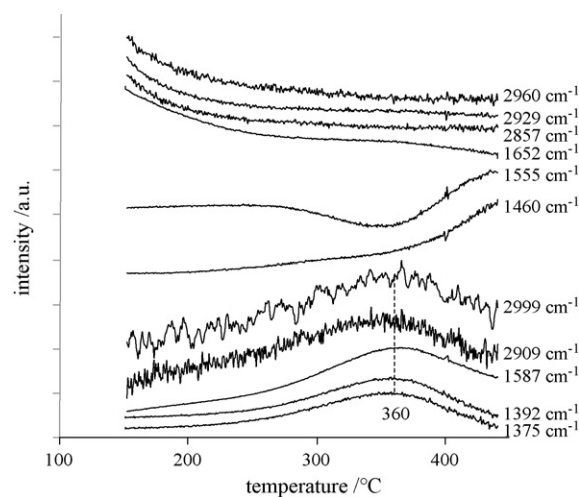
Fig. 6. Evolution of IR bands intensity of 1 wt.% Au/Al$_2$O$_3$ during temperature-programmed reaction with 467 ppm NO, 958 ppm CO, 958 ppm C$_3$H$_6$, 173 ppm C$_{10}$H$_{22}$, 5% O$_2$ and balance He.

Fig. 8. Evolution of IR bands intensity of 1 wt.% Au/Al$_2$O$_3$ during temperature-programmed reaction with 467 ppm NO, 958 ppm CO, 958 ppm C$_3$H$_6$, 173 ppm C$_{10}$H$_{22}$, 2000 ppm H$_2$, 5% O$_2$ and balance He.
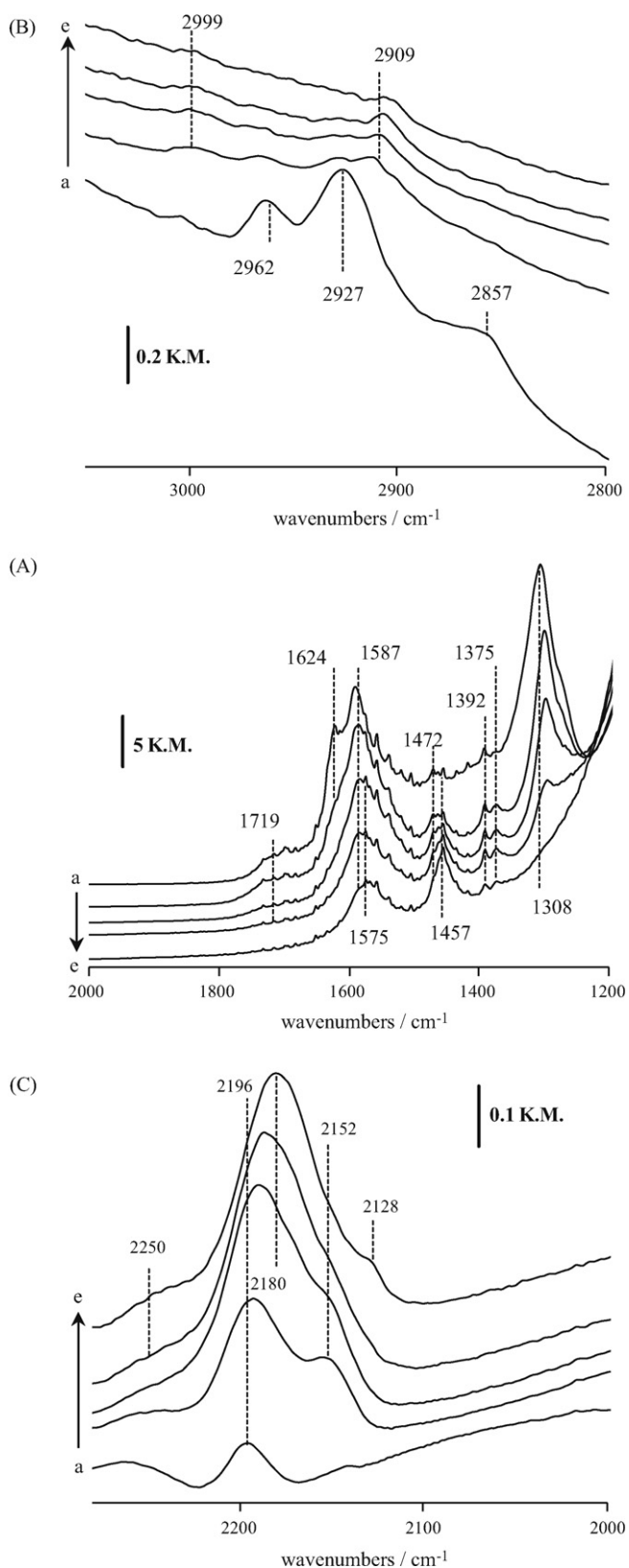
Fig. 7. IR spectra of 1 wt.% Au/Al$_2$O$_3$ in temperature-programmed conditions with 467 ppm NO, 958 ppm CO, 958 ppm C$_3$H$_6$, 173 ppm C$_{10}$H$_{22}$, 2000 ppm H$_2$, 5% O$_2$ and balance He in the 1200–1950 cm^{-1} region. (a) 130 °C, (b) 269 °C, (c) 330 °C, (d) 363 °C and (e) 409 °C.
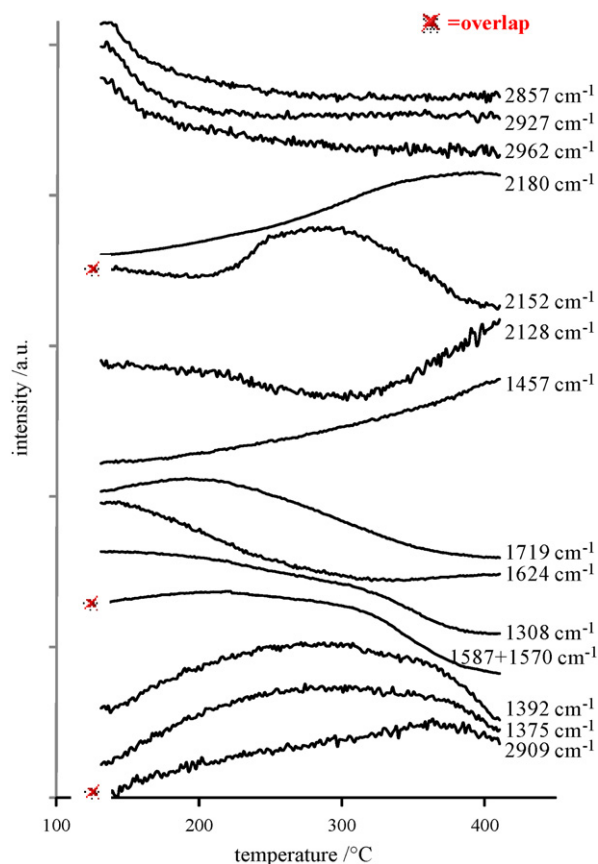
observed. The increase in temperature leads to the consumption of nitrate/nitrite adsorbed species as well as nitrosyl species and the complete disappearance of corresponding IR signals around 300 °C.

In the 2250–2000 cm^{-1} region new bands at 2196 and 2152 cm^{-1} are observed between 130 and 270 °C (Fig. 6c). Bion et al. [24] report on Ag/Al$_2$O$_3$ the presence of iso-cyanate and cyanide species at 2255–2228 cm^{-1} (Al–NCO) and 2155–2127 cm^{-1} (Ag$^+$–CN and/or Al–CN). The band at 2195 cm^{-1} can be ascribed to Au–CN species whereas the one at 2152 cm^{-1} to Al–CN. The intensity of the band at 2152 cm^{-1} decreases with increasing temperature. The band at 2195 cm^{-1} shifts to 2180 cm^{-1} with increasing temperature along with increase in the intensity. Additional band at 2128 cm^{-1} corresponding to cyanide species is observed at 409 °C. The presence of isocyanate with correspond-ing signal near 2250 cm^{-1} can be suggested at high temperature, probably due to the transformation of –CN species to –NCO species with increasing temperature. It is noteworthy that the formation of cyanide and/or isocyanate species is evidenced only in the pres-ence of hydrogen in the feed. At high temperature, spectral features assigned to formate species develop until 300 °C before diminish-ing whereas above 400 °C signals of carbonate species and nitrite species at 1457 and 1575 cm^{-1} predominate.

4. Discussion

Our results clearly demonstrate that Au/Al$_2$O$_3$ catalyst exhibits high catalytic activity for the selective reduction of NO to nitrogen with propylene, decane and hydrogen in the presence of oxy-gen and moisture. The catalyst is the most active above 350 °C with a complete selectivity towards N$_2$. Ueda et al. [9] have car-

ried out a study of gold supported on different metal oxides (α-Fe$_2$O$_3$, ZnO, MgO, TiO$_2$ and Al$_2$O$_3$) prepared by deposition-precipitation and coprecipitation methods with different gold loading (0.17–1.2 wt.%). Their reaction gas mixture consist of 1000 ppm NO, 500 ppm C$_3$H$_6$, 5% O$_2$, 1.8% H$_2$O and balance He and the space velocity used was 20,000 h^{-1}. Amongst the different supports the highest NO conversion to N$_2$ (38%) is obtained on Au/Al$_2$O$_3$ with a metal loading of 0.82 wt.% at 400 °C prepared by deposition-precipitation method. Compared to the above data, the activity of 1 wt.% Au/Al$_2$O$_3$ in the absence of H$_2$ (Fig. 1A) in this study is almost half (20% around 380 °C). This may be due to a lower NO$_x$ concentration (300 ppm NO *vs.* 1000 ppm NO), changes in the gas composition and higher space velocity which mimic the real exhaust gas conditions.

The addition of hydrogen to the feed gas strongly enhances NO reduction to N$_2$ when combined with propylene and decane, with an effect similar to the well-known activity enhancement observed on supported silver catalysts [5]. However, catalytic activity window range of Au catalyst is observed at higher temperature than the one of silver-based catalyst as illustrated in Fig. 1. The beneficial effect of H$_2$ on NO$_x$ reduction over supported gold catalysts is already known. Indeed Ueda et al. in a comparative study of NO$_x$ reduction with propane, propene, ethane and ethene in the presence of oxygen and moisture reports that the H$_2$ addition significantly improves the conversion of NO to N$_2$ in the low temperature region [11]. However, in our case, the effect of H$_2$ on the reduction of NO is limited concerning the shift of temperature range. This may be because of the presence of CO in the reaction feed, which inhibits the reaction between H$_2$ and NO$_x$ at low temperature. Macleod et al. reports that, during the lean NO$_x$ reduction with CO + H$_2$ over Pt/Al$_2$O$_3$, the surface of the catalyst is poisoned by CO due to strong adsorption and subsequent coverage by CO which in turn increases the temperature required to initiate the reaction between NO$_x$ and H$_2$ [12]. However, no CO adsorption on gold can be evidenced during our IR experiments. In another study, in order to understand the effects of H$_2$ on the SCR of NO$_x$ under diesel exhausts conditions, Abu-Jrai and Tsolakis [27] carried out H$_2$-SCR over 1 wt.% Pt/Al$_2$O$_3$ followed by simultaneous addition of CO and hydrocarbons. They report that in the presence of H$_2$ alone the NO$_x$ reduction activity peaks at 140 °C whereas in the presence of CO and hydrocarbons the maximum temperature peak shifts to higher temperatures (200–250 °C). From the above discussion it is clear that the presence of CO can be detrimental to the NO$_x$ reduction activity in the low temperature region through the accumulation of inhibiting species (carbonate, isocyanate, etc.) and suppresses the beneficial effects of H$_2$. At higher temperature, propylene and decane are the active reductants for the selective catalytic reduction of NO$_x$ by hydrocarbons. The role of H$_2$ seems strongly related to the presence of decane in the gas mixture. In the absence of decane, the SCR of NO by propylene strongly attenuates because competitive oxidation of propylene by O$_2$ predominates. After decane addition, SCR of NO involves both decane and propylene with a coincident activation. As observed, strong adsorption of decane at the surface of the catalyst, confirmed by IR experiments, can limit the competitive oxidation with a beneficial effect on SCR. In the presence of H$_2$, similar catalytic behavior is observed with simultaneous activation of decane and propylene in the temperature range of NO conversion. However, the nature of adsorbed species strongly changes after H$_2$ addition indicating a specific interaction of H$_2$ with the surface. Nevertheless, the role of adsorbed species during NO reduction in lean conditions is not well understood on supported gold catalysts.

In the absence of decane and hydrogen, formate species and carbonate/nitrite species are detected whereas no evidence of NO adsorption on gold is observed in these conditions. Lee and Schwank previously claimed that NO does not absorb on Au/SiO$_2$

and Au/MgO [28] but propylene adsorption and oxidation as formate intermediate can illustrate the reaction with oxygen and/or NO in lean conditions. The role of formate species is questionable as they are mostly considered as spectator species on alumina support [29]. Indeed in our study, the formation of formate is not promoted by hydrogen for example leading to the conclusion that formate is probably not directly involved in the reduction of NO. In the case of silver-based catalyst, isocyanate species are proposed to have a key-role in the deNO$_x$ process [24]. The formation of silver cyanide is followed by its transformation into Al^{3+}NCO adsorbed species which are hydrolysed into ammonia. Adsorbed –NH$_3$ species then further reacts stoichiometrically with NO, leading to high N$_2$ selectivity. This reaction scheme may be relevant in the case of gold-based catalysts as well. In the presence of hydrogen, cyanide species interacting with Au or Al are observed. The presence of isocyanate species adsorbed on gold can be alternately proposed with the band at 2195 cm^{-1} as proposed by Solymosi et al. [23] but the assignment is still under debate. Hydrolysis of those species can promote nitrogen formation as proposed by Bion et al. [24] although the presence of cyanide and/or isocyanate can also reflect an indirect role of hydrogen, i.e. to prevent oxygen accumulation on the surface of gold nanoparticles. However, the role of hydrogen is probably similar on Au/Al$_2$O$_3$ and in the case of silver-based catalysts despite previous studies stating that the oxidation of H$_2$ by O$_2$ arises more readily on gold catalysts than the NO$_2$ + H$_2$ reaction [11]. Indeed in this case the observation of nitrosyl species adsorbed on gold metallic nanoparticles is only an indirect indication of the alleged role of hydrogen in the prevention of oxygen accumulation on the nanoparticles.

The mechanism for the selective reduction of NO$_x$ is unclear and the nature of the active site is still under debate with various explanations involving low coordinated surface atoms [30], active sites available at the metal/support interface [31], an active ensemble of Au–OH and metallic Au atoms [32]. On the basis of these suggestions, it is also worthwhile to note that nano-sized gold particles seem to behave like silver which can emphasizes the relevance of the gold/support interface in determining the catalytic performances in the SCR of NO$_x$ by decane, as illustrated in this study. The key point is related to the effective role of H$_2$. It seems obvious that the direct NO/H$_2$ reaction is not activated on Au/Al$_2$O$_3$ as previously evidenced on Ag/Al$_2$O$_3$ [33]. In fact, the optimal catalytic performances of Au/Al$_2$O$_3$ can combine, as earlier suggested on Ag/Al$_2$O$_3$, the oxidation of NO to NO$_2$, often suggested as rate determining step for the SCR of NO$_x$ by hydrocarbons, and subsequent reaction involving NO$_2$ and/or ad-NO$_x$ species on alumina with oxygenates produced by the partial oxidation of hydrocarbons as shown from IR experiments. Returning to the formation of NO$_2$, similarly metallic particles can be involved. Despite some discrepancies on the dissociative adsorption of O$_2$ [34] it is proposed that gold particle have the ability to dissociate O$_2$ and because of its low heat of adsorption, adsorbed oxygen would be very reactive [35]. Hence, the presence of hydrogen can preserve the metallic character of gold and then favor the adsorption of NO and its subsequent reaction to produce NO$_2$ as intermediate.

5. Conclusion

The alumina supported gold catalyst shows good activity and selectivity in the reduction of NO to N$_2$ under lean conditions, although NO reduction into N$_2$ is observed at higher temperature compared to Ag/Al$_2$O$_3$ catalyst. Hydrogen does not show any promotional effect on the reduction of NO in the low temperature region. However, NO reduction promotion in the presence of hydrogen occurs at high temperatures on gold supported catalyst. A beneficial effect of H$_2$ and decane addition is evidenced for the selective catalytic reduction of NO to N$_2$. IR studies show that the

addition of hydrogen increases the formation of surface adsorbed species. Formate species evidenced at high temperature are probably not directly involved in the reduction of NO. The involvement as intermediate species of isocyanate and/or cyanide species observed mainly in the presence on decane and hydrogen is discussed and can partly explain the activity enhancement observed in the presence of H_2 and decane.

Acknowledgment

References

[1] R. Burch, J.P. Breen, F.C. Meunier, Appl. Catal. B 39 (2002) 283–303.
[2] N. Miyoshi, S. Masumoto, K. Katoh, T. Tanaka, J. Harada, SAE Technical paper, ser. No. 950809 (1995).
[3] K. Katoh, T. Kihara, T. Asanuma, M. Gotoh, N. Shibagaki, Toyota Tech. Rev. 44 (1994) 27.
[4] M. Koebel, M. Elsener, M. Kleemann, Catal. Today 59 (2000) 335–345.
[5] J.P. Breen, R. Burch, C. Hardacre, C.J. Hill, B. Krutzsch, B. Bandl-Konrad, E. Jobson, L. Cider, P.G. Blakeman, L.J. Peace, M.V. Twigg, M. Preis, M. Gottschling, Appl. Catal. B 70 (2007) 36–44.
[6] N. Jagtap, S.B. Umbarkar, P. Miquel, P. Granger, M.K. Dongare, Appl. Catal. B 90 (2009) 416–425.
[7] E. Seker, E. Gulari, Appl. Catal. A 232 (2002) 203–217.
[8] E. Seker, E. Gulari, R.H. Hammerle, C. Lambert, J. Leerat, S. Osuwan, Appl. Catal. A 226 (2002) 183–192.
[9] A. Ueda, T. Oshima, M. Haruta, Appl. Catal. B 12 (1997) 81–93.
[10] A. Ueda, M. Haruta, Appl. Catal. B 18 (1998) 115–121.
[11] A. Ueda, M. Haruta, Gold Bull. 32 (1999) 3–11.
[12] L.Q. Nguyen, C. Salim, H. Hinode, Appl. Catal. A 347 (2008) 94–99.
[13] D. Niakolas, Ch. Andronikou, Ch. Papadopoulou, H. Matralis, Catal. Today 112 (2006) 184–187.
[14] A.C. Gluhoi, S.D. Lin, B.E. Nieuwenhuys, Catal. Today 90 (2004) 175–181.
[15] L. Ilieva, G. Pantaleo, I. Ivanov, A.M. Venezia, D. Andreeva, Appl. Catal. B 65 (2006) 101–109.
[16] L. Ilieva, G. Pantaleo, J.W. Sobczak, I. Ivanov, A.M. Venezia, D. Andreeva, Appl. Catal. B 76 (2007) 107–114.
[17] M. Brandhorst, S. Cristol, M. Capron, C. Dujardin, H. Vezin, G. Le bourdon, E. Payen, Catal. Today 113 (2006) 34–39.
[18] D.A. Shirley, Phys. Rev. B 5 (1972) 4709–4714.
[19] A.-S. Mamede, L. Gengembre, E. Payen, P. Granger, G. Leclercq, J. Grimblot, Surf. Interface Anal. 34 (2002) 105–111.
[20] G. Busca, J. Lamotte, J.-C. Lavalley, V. Lorenzelli, J. Am. Chem. Soc. 109 (1987) 5197–5202.
[21] R. Greenler, J. Chem. Phys. 37 (1962) 2094–2100.
[22] F. Solymosi, T. Bansagi, J. Catal. 156 (1995) 75–84.
[23] F. Solymosi, T. Bansagi, T. Zakar, Phys. Chem. Chem. Phys. 5 (2003) 4724–4730.
[24] N. Bion, J. Saussey, M. Masaaki, M. Daturi, J. Catal. 217 (2003) 47–58.
[25] M. Kantcheva, A.S. Vakkasoglu, J. Catal. 223 (2004) 352–363.
[26] F.C. Meunier, V. Zuzaniuk, J.P. Breen, M. Olsson, J.R.H. Ross, Catal. Today 59 (2000) 287–304.
[27] A. Abu-Jari, A. Tsolakis, Int. J. Hydrogen Energy 32 (2007) 2073–2080.
[28] J.Y. Lee, J. Schwank, J. Catal. 102 (1986) 207–215.
[29] E. Iojoiu, P. Gélin, H. Praliaud, M. Primet, Appl. Catal. A 263 (2004) 39–48.
[30] F. Boccuzi, G. Cerrato, F. Pinna, G. Strukul, J. Phys. Chem. B 102 (1998) 5733–5736.
[31] M. Haruta, Catal. Today 36 (1997) 153–166.
[32] C.K. Costello, J.H. Yang, H.Y. Law, Y. Wang, J.-N. Lin, L.D. Marks, M.C. Kung, H.H. Kung, Appl. Catal. A 243 (2003) 15–24.
[33] M. Richter, U. Bentrup, R. Eckelt, M. Schneider, M.-M. Pohl, R. Fricke, Appl. Catal. B 51 (2004) 261–274.
[34] Z.-P. Liu, P. Hu, A. Alavi, J. Am. Chem. Soc. 124 (2002) 14770–14779.
[35] A.C. Gluhoi, M.A.P. Dekkers, B.E. Nieuwenhuys, J. Catal. 219 (2003) 197–205.